Radiation Environment for FIRE Diagnostic Ports

M.E. Sawan and K.M. Young

October 2003

UWFDM-1221

Presented at the 20th IEEE/NPSS Symposium on Fusion Engineering (SOFE), San Diego CA, 14-17 October 2003.

FUSION TECHNOLOGY INSTITUTE

UNIVERSITY OF WISCONSIN

MADISON WISCONSIN

Radiation Environment for FIRE Diagnostic Ports

M.E. Sawan and K.M. Young

Fusion Technology Institute
University of Wisconsin
1500 Engineering Drive
Madison, WI 53706

http://fti.neep.wisc.edu

October 2003

UWFDM-1221

Presented at the 20th IEEE/NPSS Symposium on Fusion Engineering (SOFE), San Diego CA, 14-17 October 2003.

Radiation Environment for FIRE Diagnostic Ports

M.E. Sawan, University of Wisconsin, 1500 Engineering Dr., Madison, WI 53706
K.M. Young, Princeton Plasma Physics Laboratory, P.O. Box 451, Princeton, NJ 08543

***Abstract*. Two-dimensional neutronics calculations have been performed to determine the nuclear radiation environment at selected locations in the FIRE diagnostics penetrations and to assess the impact of streaming on average flux outside the port flange. The total neutron flux (integrated over all energies), the fast neutron flux (E > 0.1 MeV) and the total gamma flux were calculated at the front of the plug, along the penetrations, at the back of the plug and at the back of the port flange. In addition, the absorbed dose rates in silica (SiO_2) and alumina (Al_2O_3) were calculated. Two types of penetrations were assessed. These are straight and 4-bend penetrations. Radiation streaming calculations indicated that the port plug should be increased to 3.4 m, the location of the cryostat interface, to ensure that the dose rates after shutdown in the area behind the port flange are similar to the acceptable levels obtained in the 1.1-m plug without penetrations.**

I. INTRODUCTION

The Fusion Ignition Research Experiment (FIRE) is in the preconceptual design phase. It utilizes 16 cryogenically cooled wedged copper TF coils with beryllium copper in the inner legs and OFHC copper in the outer legs [1]. The baseline design has a major radius of 2.14 m and an aspect ratio of 3.6. Pulses producing a total DT fusion energy of 5 TJ and DD fusion energy of 0.5 TJ are planned. The average neutron wall loading during the 150 MW DT pulses is 1.85 MW/m^2. The vacuum vessel has 16 large access ports arranged at the midplane to be used for RF heating, remote handling, and diagnostics. 1.1 m thick shield plugs plug these 1.3 x 0.7 m ports during operation. Diagnostics equipment and penetrations have to be integrated with several of these shield plugs resulting in degrading the shielding performance.

Neutron and gamma fluxes can affect plasma diagnostic performance through enhanced conductivity of electrical insulation and scintillation and absorption in optical components close to the tokamak. Determination of the radiation environment is essential for estimating shielding requirements for diagnostic components such as insulated cables, windows, fiber optics and transducers, as well as detectors and their associated electronics. In addition, streaming through diagnostics penetrations could lead to excessive doses outside the machine.

In FIRE, a few diagnostics, such as the neutral particle analyzer (NPA) and impurity pellet guide tubes require straight holes through the port shielding plugs. Other diagnostics, notably optical systems such as Thomson scattering, will make use of labyrinthine penetrations to curtail the streaming. Such penetrations will include four bends with mirrors at the corners. A schematic of the diagnostics and penetrations in the midplane diagnostics port plug J is shown in Fig. 1. This port was identified as the most critical diagnostic port that requires special attention regarding radiation shielding. Two-dimensional neutronics calculations have been performed to determine the nuclear radiation environment at selected locations in the diagnostics penetrations and to assess the impact of streaming on the average flux outside the port flange.

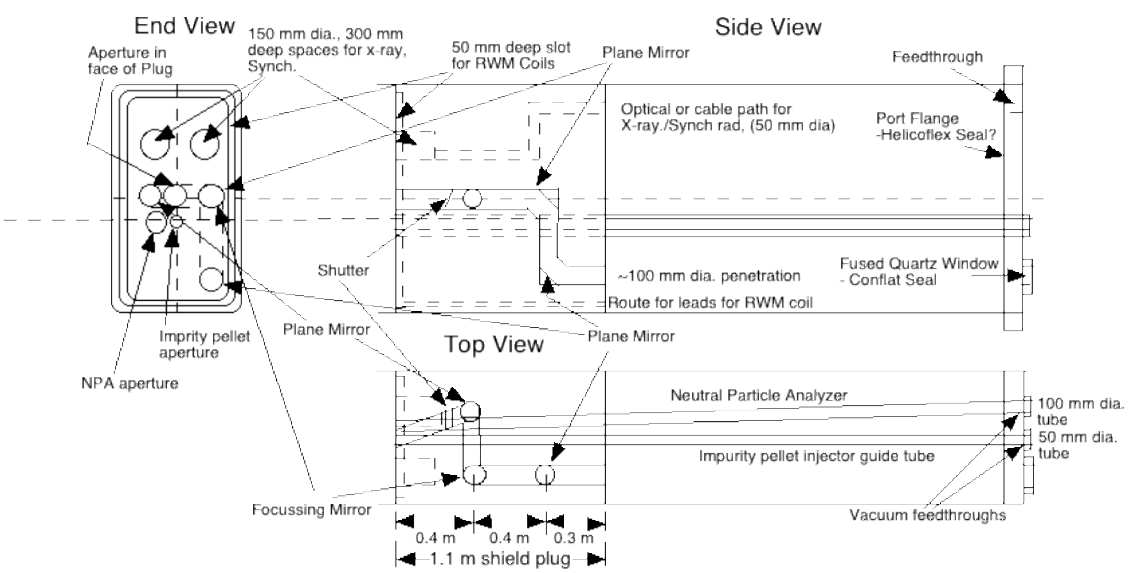

Fig. 1. Schematic of diagnostics and penetrations in port plug J.

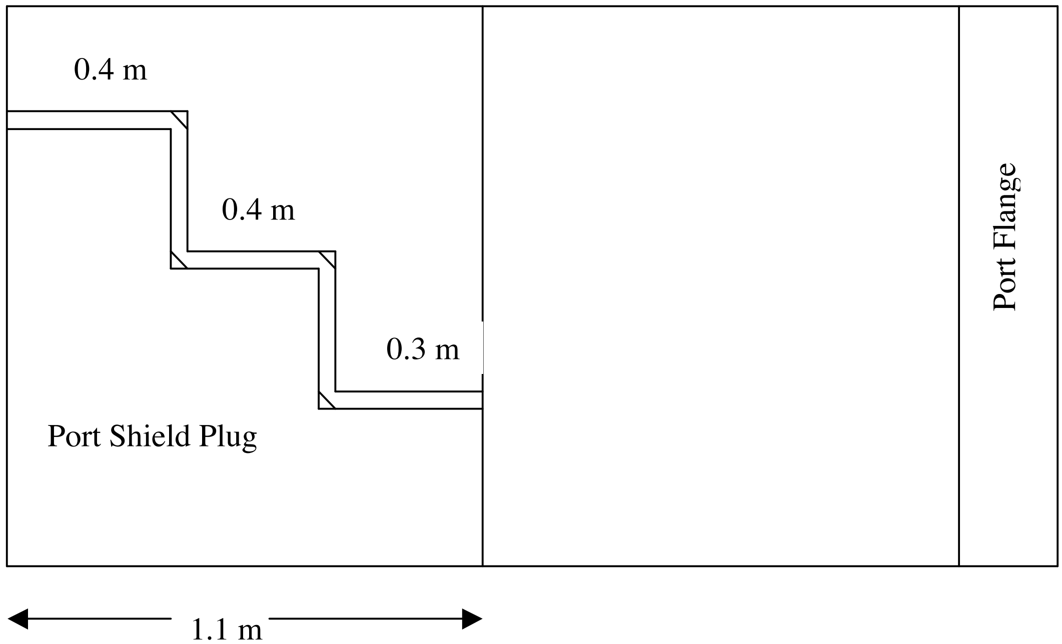

Fig. 2. Two-dimensional model used for the Thomson scattering penetration.

II. Calculation Procedure

The neutronics calculations have been performed using the two-dimensional module of the DANTSYS neutral particle transport code [2] with the most recent FENDL-2 nuclear evaluated data [3]. A simplified geometry was modeled in r-z cylindrical geometry. In the model both the inboard and outboard regions are modeled simultaneously to properly account for the toroidal geometry effects. The calculations were performed for the DT pulses with 150 MW fusion power using the midplane radial build for the FIRE machine with 2.14 m major radius. The front of the 110 cm thick port plug facing the plasma is at a radius of 282.2 cm. The radial distance between the front of the port plug and the 2.5 cm thick port flange is 339 cm. The port plug and flange are assumed to consist of 80% steel and 20% water. Three different models were used in the calculations. The first one assumes no penetrations in the plug and flange. The results from this calculation are used as a reference to quantify the impact of streaming. The second case considered is for the worst case streaming with a 10 cm straight penetration through the plug and flange. This is representative of the NPA tube. The third case includes a penetration with four bends and represents the Thomson scattering laser well. Due to the limitation of two-dimensional modeling, all bends were modeled in the same plane as shown in Fig. 2. Notice that conservative estimates are obtained using these two-dimensional models since the penetrations are modeled as slots that extend toroidally and attenuation by components in the penetrations is not included. The total neutron flux (integrated over all energies), the fast neutron flux (E > 0.1 MeV) and the total gamma flux were calculated at the front of the plug, along the penetrations, at the back of the plug and at the back of the port flange. In addition, the absorbed dose rates in silica (SiO_2) and alumina (Al_2O_3), were calculated. This includes the contributions from both neutrons and gammas. The gamma contribution to the dose varies from ~30% at the front of the port plug to ~80% at the back of the port flange.

III. Nuclear Environment in Diagnostics Penetrations

Table I gives the neutron and gamma fluxes for the case without penetrations at the front of the port plug, at the back of the plug and at the back of the port flange. The fluxes attenuate by about seven orders of magnitude in the shield plug. For the case with a straight penetration the neutron and gamma fluxes along the penetration are given in Table II. In addition, the average values at the three radial locations are provided. At the back of the port plug, a flux peaking factor of ~7 occurs due to the penetration. At the back of the flange the peaking factor is only ~4 following neutron and gamma transport in the large void space between the plug and flange. Notice that the average flux values behind the plug and flange are about four orders of magnitude higher than those in the case without the penetration. Hence, using a straight penetration in the port plug increases the radiation environment in the test cell area behind the flange by about four orders of magnitude. This implies also that the biological dose rate will increase accordingly.

For the Thomson scattering penetration with four bends, the fluxes and absorbed dose rates were calculated at the mirrors located at each of the bends. In addition, results are given at the front of the plug, back of the plug, and back of the flange. Table III lists the neutron and gamma fluxes along the penetration. The average values at the back of the plug and at the back of the flange are given in Table IV. At the back of the plug, the peak values occur at the exit of the penetration with a peaking factor of ~4. Since the penetration does not go through the port flange, the peaking factor behind the flange is only ~2. The average flux values behind the plug and the flange are about a factor of 200 higher than those without penetrations. Hence, the presence of the 4-bend penetration results in enhancing the radiation fluxes and dose rates in the test cell area by about two orders of magnitude. Diagnostic equipment in the penetration will reduce this enhancement. Table V gives the absorbed dose rates in silica and alumina along the 4-bend penetration and at the back of the port flange. The dose rates in the 4-bend penetration at the back of the port plug are about two orders of magnitude less than with a straight penetration.

TABLE I
NEUTRON AND GAMMA FLUXES DURING 150 MW DT FUSION POWER PULSES FOR PORT PLUG WITHOUT PENETRATIONS

	Total Neutron Flux (n/cm^{2}s)	Fast Neutron Flux (E>0.1 MeV) (n/cm^{2}s)	Total Gamma Flux (□/cm^{2}s)
Front of port plug	8.38x10^{14}	5.85x10^{14}	4.94x10^{14}
Back of port plug	3.51x10^{7}	1.64x10^{7}	3.04x10^{7}
Back of port flange	1.04x10^{7}	6.23x10^{6}	1.04x10^{7}

TABLE II
NEUTRON AND GAMMA FLUXES FOR THE CASE OF STRAIGHT 10 CM PENETRATION

	Total Neutron Flux (n/cm^{2}s)		Fast Neutron Flux (E>0.1 MeV) (n/cm^{2}s)		Total Gamma Flux (□/cm^{2}s)	
	Along Penetration	Average	Along Penetration	Average	Along Penetration	Average
Front of port plug	7.46x10^{14}	8.38x10^{14}	5.34x10^{14}	5.85x10^{14}	4.14x10^{14}	4.94x10^{14}
Back of port plug	2.87x10^{12}	4.06x10^{11}	1.28x10^{12}	1.57x10^{11}	2.08x10^{12}	2.79x10^{11}
Back of port flange	5.14x10^{11}	1.27x10^{11}	2.75x10^{11}	6.38x10^{10}	3.96x10^{11}	1.03x10^{11}

TABLE III
NEUTRON AND GAMMA FLUXES DURING 150 MW DT FUSION POWER PULSES FOR THE 4-BEND PENETRATION

	Total Neutron Flux (n/cm^{2}s)	Fast Neutron Flux (E>0.1 MeV) (n/cm^{2}s)	Total Gamma Flux (□/cm^{2}s)
Entrance at front of port plug	7.48x10^{14}	5.34x10^{14}	4.15x10^{14}
First bend	1.20x10^{14}	6.24x10^{13}	7.68x10^{13}
Second bend	2.06x10^{13}	7.95x10^{12}	1.37x10^{13}
Third bend	2.57x10^{12}	9.19x10^{11}	1.79x10^{12}
Fourth bend	2.87x10^{11}	6.75x10^{10}	2.15x10^{11}
Exit at back of port plug	2.92x10^{10}	6.82x10^{9}	2.46x10^{10}
Peak at back of port flange	5.00x10^{9}	1.50x10^{9}	5.00x10^{9}

TABLE IV
AVERAGE NEUTRON AND GAMMA FLUXES AT BACKS OF PLUG AND FLANGE WITH A PENETRATION WITH 4 BENDS

	Total Neutron Flux (n/cm^{2}s)	Fast Neutron Flux (E>0.1 MeV) (n/cm^{2}s)	Total Gamma Flux (□/cm^{2}s)
Back of port plug	6.98x10^{9}	2.26x10^{9}	5.97x10^{9}
Back of port flange	1.99x10^{9}	8.84x10^{8}	2.10x10^{9}

TABLE V
ABSORBED RADIATION DOSE RATE IN SILICA AND ALUMINA ALONG THE 4-BEND PENETRATION

	Dose Rate During 150 MW DT Pulses (Rad/s)	
	Silica	Alumina
Front of port plug	7.90x10^{5}	8.48x10^{5}
First bend	7.69x10^{4}	9.85x10^{4}
Second bend	1.01x10^{4}	1.76x10^{4}
Third bend	1.24x10^{3}	2.25x10^{3}
Fourth bend	1.41x10^{2}	2.67x10^{2}
Back of port plug	1.65x10^{1}	3.14x10^{1}
Back of port flange	3.80	7.07

Figure 3 shows the vertical distribution of the fast neutron flux at the back of the port plug for the three cases considered. While the flux is nearly uniform for a plug without any penetrations, using a straight penetration results in significant peaking at the exit of the penetration. For the penetration with 4 bends, the flux peaks at the exit of the penetration with a small local peaking behind the third bend. The figure indicates also the relative enhancement in the average flux level behind the port plug resulting from these penetrations.

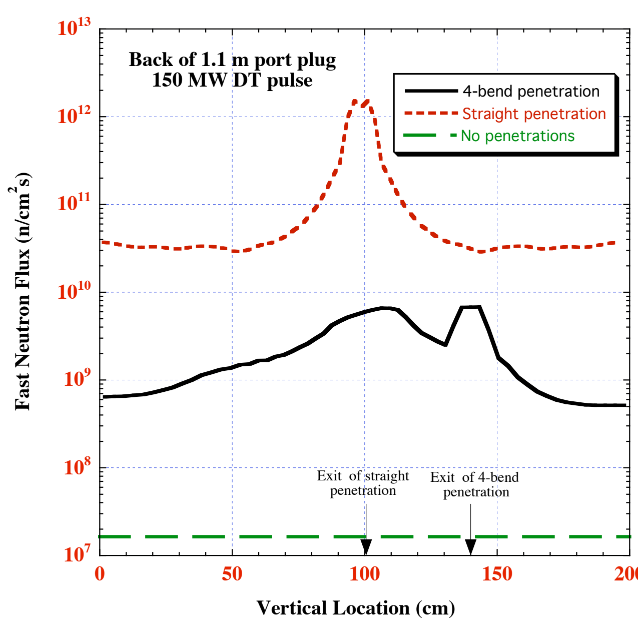

Fig. 3. Spatial distribution of fast neutron flux behind the port plug.

TABLE VI
NEUTRON AND GAMMA FLUXES AT THE BACK OF THE PORT FLANGE DURING 150 MW DT FUSION POWER PULSES WITH DIFFERENT PLUG THICKNESSES

	Total Neutron Flux (n/cm^{2}s)		Fast Neutron Flux (E>0.1 MeV) (n/cm^{2}s)		Total Gamma Flux (γ/cm^{2}s)	
	Peak	Average	Peak	Average	Peak	Average
1.1 m plug without penetrations	1.04×10^7	1.04×10^7	6.23×10^6	6.23×10^6	1.04×10^7	1.04×10^7
1.1 m plug with 10 cm straight penetration	5.14×10^{11}	1.27×10^{11}	2.75×10^{11}	6.38×10^{10}	3.96×10^{11}	1.03×10^{11}
3.4 m plug with 10 cm straight penetration	4.18×10^7	2.64×10^6	1.08×10^7	7.51×10^5	4.28×10^7	2.96×10^6
1.1 m plug with 10 cm 4-bend penetration	5.00×10^9	1.99×10^9	1.50×10^9	8.84×10^8	5.00×10^9	2.10×10^9
3.4 m plug with 10 cm 4-bend penetration	9.64×10^4	7.04×10^3	1.97×10^4	1.63×10^3	1.59×10^5	1.33×10^4

IV. ADDITIONAL SHIELDING REQUIREMENT

Since the flux values in the test cell area behind the port flange are increased significantly due to streaming, the biological dose rate will be enhanced, affecting the accessibility for hands-on clearing services prior to removal/installation of port assemblies by remote handling means. Acceptable biological dose rates behind the port flange were obtained from activation calculations performed with a 1.1 m port plug without any penetrations [4]. These dose rates are ~10 mrem/hr at shutdown, ~3 mrem/hr after 1 hr, ~0.1 mrem/hr after 1 day, and about 0.05 mrem/hr after 1 week. These acceptable dose rates can be maintained in the cases where penetrations are employed in the shield plug by increasing the plug thickness. Past activation calculations indicated that the dose rate scales linearly with the total neutron flux provided the material used in the area where the dose is calculated is not changed. We performed two-dimensional neutronics calculations with different plug thicknesses for the cases with straight and 4-bend penetrations. Table VI gives the results for the 1.1 m plug and for the case where all the port is filled by the plug. The peak and average flux levels are shown behind the port flange. The results for the 1.1 m plug without penetrations are included for comparison. For the straight penetration, the flux peaking factor increases from ~4 with the 1.1 m plug to ~15 with the 3.4 m plug. On the other hand, for the 4-bend penetration, the flux peaking factor increases from ~2 with the 1.1 m plug to ~13 with the 3.4 m plug. The average neutron flux behind the flange decreases by an order of magnitude by making the shield plug with the straight penetration thicker by ~0.5 m. The same drop in flux is obtained by a ~0.42 m thicker plug for the case with 4-bend penetration. The results imply that if a straight 10 cm penetration is employed in the port plug, the plug thickness needs to be increased to ~3.1 m to ensure that the dose rates after shutdown in the area behind the port flange are similar to the acceptable levels obtained without penetrations. For the case with the 4-bend penetration employed, the plug thickness should be increased to ~2.1 m. Since both penetrations exist in the diagnostic port J, it is recommended that the port plug thickness should be increased to 3.4 m, the location of the cryostat interface.

V. SUMMARY AND CONCLUSIONS

Two-dimensional neutronics calculations have been performed for the FIRE diagnostics port that employs straight and labyrinthine penetrations in the port shield plug. These penetrations are representative of the neutral particle analyzer and Thomson scattering penetrations. The nuclear radiation environment at selected locations in the diagnostics penetrations was determined. The total neutron flux (integrated over all energies), the fast neutron flux (E > 0.1 MeV) and the total gamma flux were calculated at the front of the plug, along the penetrations, at the back of the plug and at the back of the port flange. In addition, the absorbed dose rates in silica (SiO_2) and alumina (Al_2O_3) were calculated. We also assessed the impact of streaming through these penetrations on the average flux level outside the port flange in the test cell area. For a 1.1 m shield plug, the straight penetration increases the average flux by about four orders of magnitude. On the other hand, the average flux increases by two orders of magnitude when the 4-bend penetration is employed. Radiation streaming calculations indicated that the port plug should be increased to 3.4 m, the location of the cryostat interface, to ensure that the dose rates after shutdown in the area behind the port flange are similar to the acceptable levels obtained for the 1.1-m plug without penetrations.

ACKNOWLEDGMENT

Support for this work was provided by the U.S. Department of Energy.

REFERENCES

[1] D.M. Meade, "FIRE, a Next Step Option for Magnetic Fusion," Fusion Engineering and Design, vol. 63-64, pp. 531-540 (2002).

[2] R.E. Alcouffe et al., "DANTSYS 3.0, One-, Two-, and Three-Dimensional Multigroup Discrete Ordinates Transport Code System," RSICC Computer Code Collection CCC-547, Contributed by Los Alamos National Lab, August 1995.

[3] M. Herman and H. Wienke, "FENDL/MG-2.0 and FENDL/MC-2.0, The Processed Cross-Section Libraries For Neutron-Photon Transport Calculations," Report IAEA-NDS-176, International Atomic Energy Agency (1997).

[4] M. Sawan, H. Khater and S. Zinkle, "Nuclear Features of the Fusion Ignition Research Experiment (FIRE)," Fusion Engineering and Design, vol. 63-64, pp. 547-557 (2002).